Locating the rate-limiting step for the interaction of hydrogen with Mg(0001) using density-functional theory calculations and rate theory

Tejs Vegge[1,2]
[1]*CAMP and Department of Physics, Technical University of Denmark, DK-2800 Kgs. Lyngby, Denmark*
[2]*Danfoss Corporate Ventures A/S, DK-6430 Nordborg, Denmark*
(Received 4 December 2003; revised manuscript received 2 March 2004; published 20 July 2004)

The dissociation of molecular hydrogen on a Mg(0001) surface and the subsequent diffusion of atomic hydrogen into the magnesium substrate is investigated using Density Functional Theory (DFT) calculations and rate theory. The minimum energy path and corresponding transition states are located using the nudged elastic band method, and rates of the activated processes are calculated within the harmonic approximation to transition state rate theory, using both classical and quantum partition functions based atomic vibrational frequencies calculated by DFT. The dissociation/recombination of H_2 is found to be rate-limiting for the ab- and desorption of hydrogen, respectively. Zero-point energy contributions are found to be substantial for the diffusion of atomic hydrogen, but classical rates are still found to be within an order of magnitude at room temperature.

DOI: 10.1103/PhysRevB.70.035412 PACS number(s): 68.43.−h, 71.15.Mb, 82.20.−w

I. INTRODUCTION

The applicability of metal hydrides as hydrogen storage media (i.e., specifically for the automotive industry) has been investigated intensely for many years.[1] With a reversible storage capacity of 7.6 wt.% and low cost, magnesium would be an ideal solid storage medium if not for a slow absorption kinetics and an elevated hydride decomposition temperature.[2] The kinetics are primarily believed to be limited by either a poor dissociative chemisorption of H_2 or a highly stable surface hydride film blocking the diffusion of atomic hydrogen into the magnesium, but no consensus has been reached.[3]

Given the vast potential applications, only relatively few investigations of the dissociation of H_2 on magnesium have been carried out. Nørskov *et al.* have performed calculations using a jellium based model finding a chemisorbed molecular precursor state and an activation energy of ~0.5 eV for H_2 dissociation on Mg(0001).[4] Bird *et al.* have performed LDA calculations, determining the bridge site to be favored for H_2 dissociation, yielding a barrier of 0.4 eV for dissociation.[5]

Experimentally, Plummer and Sprunger have used EELS and TDS to study the interaction between both atomic and molecular hydrogen and Mg, finding dissociation and adsorption to be activated; a strongly chemisorbed surface hydride state was also observed.[6,7]

The diffusional properties of hydrogen in magnesium have been investigated by Renner and Grabke, who determined a diffusion constant of $D=4.0\times10^{-13}$ m^2/s at 300 K.[8] Using neutron scattering, Töpler *et al.* found H-diffusion in MgH_2 to be three orders of magnitude lower than in Mg (at 350 K),[9] and Spatz *et al.* have determined the overall hydrogen diffusion coefficient for the Mg-to-MgH_2-transition (including nucleation and growth) to be as low as $D'=1.1\times10^{-20}$ m^2/s using XPS.[10]

In the present work, a comprehensive investigation of the potential energy surface (PES) of hydrogen on the magnesium(0001) surface is presented. Rates of activated dissociative and diffusional processes are calculated using a combination of DFT calculations, path techniques and vibrational frequencies, enabling a direct determination of the rate-limiting processes.

II. CALCULATIONAL SETUP

The electronic structure calculations in this paper are performed within DFT using the DACAPO pseudopotential implementation.[11,12] A plane wave expansion of the Kohn-Sham wavefunctions is performed up to a kinetic energy cutoff-value of 25 Ry, and 45 Ry was used as a cutoff for the density grid. Ultra-soft pseudopotentials[13] are used to describe the ionic cores, and the exchange and correlation effects are described using the RPBE functional.[14] The *k*-point sampling of the first Brillouin zone is performed with a (4,4,1) Monkhorst-Pack grid,[15] having 3-dimensional periodic boundary conditions.

The self-consistent electron density is determined by iterative diagonalization of the Kohn-Sham Hamiltonian, and the resulting Kohn-Sham eigenstates are populated following a Fermi distribution ($k_BT=0.2$ eV); Pulay mixing[16] of the resulting electronic density is subsequently performed, and finally, all total energies are extrapolated to zero temperature.

The magnesium surface is modeled using a (2×2) surface with 5 Mg(0001) layers in the super cell (see Fig. 1). A relatively thick Mg-layer is necessary in order to accommodate an expansion of the first surface layers,[17] and an additional 18 Å vacuum layer is placed between the slabs to ensure separation, resulting in a super cell of 31.2 Å in the *z*-direction.

A lattice constant of $a=3.19$ Å—determined for bulk magnesium—was used in the setup; and in all calculations, the structure is optimized by allowing the atoms to relax their atomic coordinates, keeping the surface unit cell fixed.

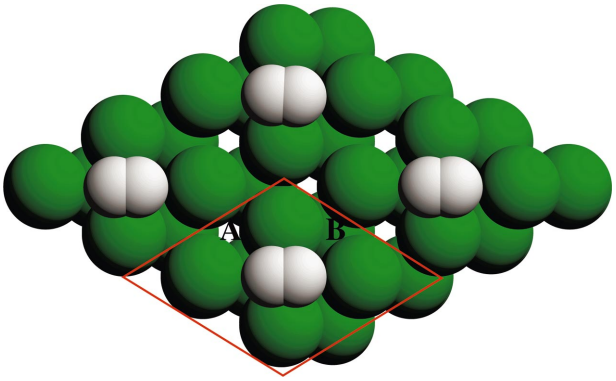

FIG. 1. (Color) The transition state for the dissociation of a hydrogen molecule (white) on a Mg(0001) surface (green). The 2 $\times$2 supercell (red) consists of 5 closed packed (0001) layers. The adsorption sites "A" (octahedral) and "B" (tetrahedral) are termed fcc- and hcp-sites, respectively.

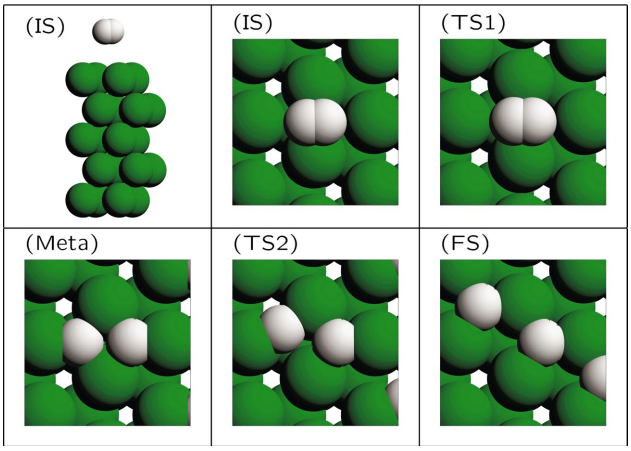

FIG. 2. (Color) The dissociation pathway for a hydrogen molecule on a Mg(0001) surface. The corresponding activation energy as a function of the reaction coordinate is found in Fig. 3.

III. METHODS

Transition state theory (TST)[18]—which is subsequently used to determine rates of activated processes within the harmonic approximation using both classical and quantum partition functions—is described in the following. Two calculational techniques: the nudged elastic band method and a vibrational analysis tool, are also introduced.

A. Transition state theory

The applicability of the Arrhenius law—and the appropriate determination of activation energies and rate-prefactors—has been dealt with in some detail in the case of atomic diffusion processes involving a few metal atoms; where an Arrhenius expression for the diffusion rate, r, is given by

$$r = \nu \exp(-E_a/k_B T). \tag{1}$$

This expression is also representative of the simplest, classical, harmonic approximation (hTST) to the general transition state expression:[18]

$$r_{\mathrm{TST}} = \frac{k_B T}{h}\frac{q_{\mathrm{TS}}}{q_{\mathrm{IS}}}\exp(-\Delta E_a/k_B T), \tag{2}$$

where q_{IS} and q_{TS} are the partition functions of the initial state (IS) and the transition state on the dividing surface (TS), respectively.

In Eq. (1), the activation energy E_a is identified as the difference in energy between TS and IS. In order to calculate the rate, it is therefore necessary to locate the transition state (i.e., the saddle point on the potential energy surface), which is done using the nudged elastic band method (see Sec. III B).

In hTST the prefactor, ν, is independent of temperature, since the temperature dependence in the partition functions scales out, and thus ν depends solely on the frequencies, ω_i, of the eigenmodes at TS and IS:

$$\nu = \frac{1}{2\pi}\frac{\prod_i \omega_i^{\mathrm{IS}}}{\prod_i' \omega_i^{\mathrm{TS}}}, \tag{3}$$

where the prime indicates that the mode with imaginary frequency corresponding to the reaction coordinate has been left out of the product over the TS modes.

It is, however, questionable, whether the simplified classical expression,

$$r_{\mathrm{cl.}} = \frac{1}{2\pi}\frac{\prod_i \omega_i^{\mathrm{IS}}}{\prod_i' \omega_i^{\mathrm{TS}}}\exp(-E_a/k_B T), \tag{4}$$

provides an accurate representation of the hydrogen processes investigated here?

The harmonic approximation should only be expected to work well at sufficiently low temperatures, where all modes can be considered harmonic (excluding possible quantum effects at very low temperatures), but several studies have shown that it is often applicable even at rather high temperatures[19,20] and in highly complex systems.[21]

The quantum nature of the hydrogen atoms must also be considered. The desorption of hydrogen from MgH_2 only occurs readily at temperature above 300 °C, where quantum tunneling is no longer significant (above the cross-over temperature), but the quantization of levels could still be important.

By inserting the quantum mechanical partition functions for the harmonic oscillator:

$$q_{\mathrm{osc}} = \sum_{n=0}^{\infty}\exp\left(-\left(n+\frac{1}{2}\right)\frac{\hbar\omega}{k_B T}\right) = \prod_i \frac{\exp\left(\frac{-\hbar\omega_i}{2k_B T}\right)}{1-\exp\left(\frac{-\hbar\omega_i}{k_B T}\right)}; \tag{5}$$

in Eq. (2), a quasi-classical expression for the rate is given by

$$r_q = \frac{k_B T}{h} \frac{\prod_i' \frac{\exp(-\hbar\omega_i^{TS}/2k_B T)}{1-\exp(-\hbar\omega_i^{TS}/k_B T)}}{\prod_i \frac{\exp(-\hbar\omega_i^{IS}/2k_B T)}{1-\exp(-\hbar\omega_i^{IS}/k_B T)}} \exp\left(\frac{-\Delta E}{k_B T}\right)$$

$$= \frac{k_B T}{h} \frac{\prod_i 1-\exp(-\hbar\omega_i^{IS}/k_B T)}{\prod_i' 1-\exp(-\hbar\omega_i^{TS}/k_B T)} \exp\left(\frac{-\Delta E^*}{k_B T}\right), \quad (6)$$

where ΔE^* is the change in ground state and zero-point energy (see Sec. V).

For the dissociation of H_2, the initial state involves a light molecule isolated from the Mg(0001) surface, thus requiring special treatment. The linear H_2 molecule has one vibrational, three translational, and two rotational degrees of freedom. The frequency, ω^{H_2}, in the vibrational partition function must be calculated to determine the zero-point energy contribution (see Sec. III C), and the rotational and translational part of the IS partition function depend on the pressure, P, and the temperature, T:[22]

$$q_{H_2} = \frac{\exp\left(\frac{-\hbar\omega^{H_2}}{2k_B T}\right)}{1-\exp\left(\frac{-\hbar\omega^{H_2}}{k_B T}\right)} \frac{k_B T}{2\epsilon_{rot}} \frac{k_B T}{P} \left(\frac{2\pi m k_B T}{h^2}\right)^{3/2}$$

$$\simeq \exp\left(\frac{-\hbar\omega^{H_2}}{2k_B T}\right) \frac{k_B T}{2\epsilon_{rot}} \frac{k_B T}{P} \left(\frac{2\pi m k_B T}{h^2}\right)^{3/2}, \quad (7)$$

where the denominator in the vibrational partition function is set to unity (does not contribute significantly at moderate temperatures), and $\epsilon_{rot}=7.55$ meV is the rotational constant for H_2.

The rate of H_2 dissociation can therefore be expressed as a function of ω_i, P and T:

$$r_{H_2} = \frac{k_B T}{h} \frac{q_{TS}}{q_{H_2}} \exp(-\Delta E/k_B T)$$

$$= \frac{k_B T}{h q_{H_2}} \prod_i' \frac{\exp(-\hbar\omega_i^{TS}/2k_B T)}{1-\exp(-\hbar\omega_i^{TS}/k_B T)} \exp(-\Delta E/k_B T)$$

$$= \frac{2h^2 \epsilon_{rot} P}{k_B T (2\pi m k_B T)^{3/2}} \frac{\exp(-\Delta E^*/k_B T)}{\Pi_i' 1-\exp(-\hbar\omega_i^{TS}/k_B T)}, \quad (8)$$

where ΔE^* is the change in ground state and zero-point energy.

The flux of hydrogen molecules hitting the surface is $F = P/\sqrt{2\pi m k_B T}$ and the area per bridge site is $A=3.02$ Å^2, resulting in a probability of dissociative sticking:

$$\sigma_{diss.} = \frac{\epsilon_{rot} h^2}{A\pi m (k_B T)^2} \frac{\exp(-\Delta E^*/k_B T)}{\prod_i' 1-\exp(-\hbar\omega_i^{TS}/k_B T)}. \quad (9)$$

The frequencies, ω_i, of the eigenmodes are determined using the vibrational analysis tool described in Sec. III C, and the rates will be calculated using both the classical [Eq. (4)] and the quasi-classical expressions [Eq. (9)].

B. The nudged elastic band method

The nudged elastic band (NEB) method is used to determine the energy barriers for the activated processes on the potential energy surface.[23] The method locates the TS between relaxed initial, e.g., the H_2 molecule far above the Mg(0001) surface, and final (a dissociated molecule on the surface) states. The transition path is represented computationally by a sequence of 11–23 configurations (images) between the initial (IS) and final state (FS), which are connected with spring forces in order to ensure continuity along the path; here, a linear interpolation in all atomic coordinates is used as an initial guess. The path is subsequently relaxed to a so-called minimum energy path (MEP), where the force perpendicular to the path vanishes. The saddle point configuration (TS), i.e., the configuration with maximal energy along the MEP, is located via the Climbing Image implementation of the NEB method.[24]

By varying the spring constants, an increased resolution can be obtained in areas of special interest, e.g., near the TS, for a detailed description see Vegge *et al.*[25]

C. Vibrational analysis tool

Entropic contributions to the rate of activated processes are known to be particularly important for hydrogen, and the large zero-point vibrations in the molecule make it necessary to include this effect in calculations of, e.g., the H_2 dissociation barrier.[26]

The vibrational frequencies are calculated with DFT, using a module in the CamposASE distribution.[27] On the basis of a converged DFT calculation, the normal modes and frequencies of specific atoms in the super cell are determined using a centered, finite difference method to calculate the elements of the Hessian matrix—within the harmonic oscillator approximation. Once the Hessian matrix is determined, it is mass-weighted and diagonalized to obtain the eigenvalues and eigenvectors, which are subsequently converted to frequencies.

For a local energy minimum, all frequencies are real, whereas for a transition state, a single imaginary frequency will appear, thus identifying the position on the potential energy surface as a saddle point, i.e., a transition state.

IV. H_2 DISSOCIATION ON Mg(0001)

Magnesium is known to be kinetically slow when reacting with hydrogen. It is, however, still unclear if this is primarily due to a poor ability to dissociate H_2 or to the creation of a stable surface hydride structure limiting the diffusion of atomic hydrogen into the Mg-matrix. Using the NEB method, the MEP and corresponding transition state is located between an initial configuration [an H_2 molecule >5 Å above a relaxed Mg(0001) surface], and a dissociated H_2 molecule, with the hydrogen atoms in two neighboring fcc sites (IS and FS, respectively, in Fig. 2). Following the reaction coordinate (see Fig. 3), the transition state for dissociation (TS_1) is found to be in the bridge site—in agreement with the findings of Bird *et al.*,[5] but yielding a substantially

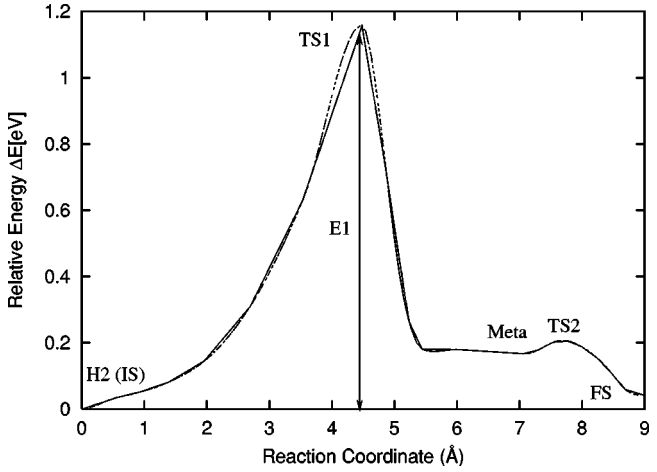

FIG. 3. The barrier for dissociation of a H_2 molecule on a Mg(0001) surface as a function of the reaction coordinate (Å). The NEB simulation consists of 21 images, and the spline-fit includes the forces to determine the gradients at each point.

higher activation energy of $E_1=1.15$ eV. A lower LDA barrier is expected, as a consequence of the LDA overbinding,[28] which is particularly pronounced in calculations, where bonds are broken and reformed for light atoms. It should also be noted that no chemisorbed molecular state was observed in the calculation.

The local minimum in Fig. 3 around 7 Å ("Meta") corresponds to the hydrogen atoms being in neighboring hcp and fcc sites (see Fig. 1); TS_2 corresponds to the barrier for moving one H-atom from an hcp to a fcc site. A barrier of only $E_2=E_{TS_2}-E_{Meta}=0.039$ eV means the atoms will quickly diffuse to separated fcc sites, given the height of E_1. The relevant barrier for recombination in connection with desorption is therefore $E_{-1}=E_{TS_1}-E_{FS}=1.11$ eV. This value is in good agreement with the experimental TDS results by Sprunger and Plummer, who found $E_{des}\simeq 1$ eV. [6]

The isolated H_2 molecule is found to have a vibrational frequency of $\omega^{H_2}=4472$ cm^{-1} corresponding to a zero-point energy of 0.277 eV (in accordance with literature values[29,26]). In TS_1 and TS_2 (Figs. 2 and 3), one mode is imaginary, corresponding to the reaction coordinate on the MEP.

In the "Meta" configuration, the hydrogen atoms are in neighboring fcc and hcp sites, which are distorted by the short H−H separation. Consequently, the normal modes are affected, and two of the modes are strongly anti-/symmetrically coupled (ω_x in Table I). The short separation between the identical fcc sites in FS causes all six of these modes to be anti-/symmetrically coupled (Table I). An average value in FS of 88 meV agrees well with EELS spectra from Sprunger and Plummer, having an energy loss at 92 meV for hydrogen in three-fold hollow sites.[7] All atomic hydrogen frequencies are listed in Table I, whereas the frequency shifts observed for the substantially heavier magnesium atoms are found to be negligible and will henceforth be disregarded.

The total change in the zero-point energy between the initial and final states are seen to be minimal, but as high as 75 meV between IS and TS_1, thus affecting the activation barrier.

TABLE I. The calculated vibrational frequencies for the IS, TS_1, Meta, TS_2, and FS for the dissociation of H_2 on Mg(0001), where **Im** indicates the imaginary frequency of the reaction coordinate. The two ω_x frequencies in Meta are anti- and symmetrically coupled, respectively, as are all the FS states. The zero-point energies are listed in the last column (eV).

	ω_x(cm^{-1})	ω_y(cm^{-1})	ω_z(cm^{-1})	$\frac{1}{2}\Sigma_i\ \omega_i$(eV)
H_2	4472			
				0.277
TS_1	**Im**	799	770	
	718	594	376	0.202
Meta(fcc)	1302/993	732	561	
Meta(hcp)	1302/993	650	424	0.289
TS_2	1213	934	**Im**	
	693	605	523	0.246
FS(fcc-anti)	747	724	680	
FS(fcc-sym)	728	697	663	0.262

V. HYDROGEN DIFFUSION IN MG(0001)

Experimental data on individual atomic diffusion processes is scarce due to the complexity involved in isolating the individual events. Much insight can therefore be gained from simulations, especially from high accuracy methods like DFT.

Jacobson *et al.*[30] have recently investigated the diffusion of a single hydrogen atom through the *fcc-channel* (channel

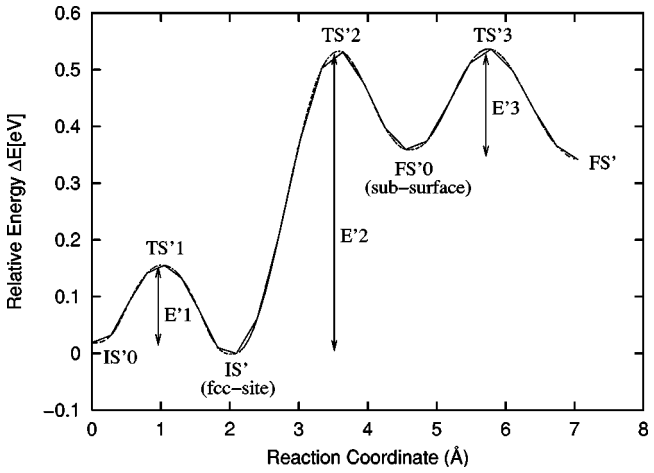

FIG. 4. The barrier for hydrogen diffusion from the hcp to the fcc site, and onward down the "fcc-channel," as a function of the reaction coordinate (Å). The NEB-simulation consist of 25 images located between IS_0' and FS′, passing three transition states (TS_1', TS_2', and TS_3').

TABLE II. The calculated vibrational frequencies for the hydrogen atom (cm^{-1}), where **Im** indicates the imaginary frequency of the reaction coordinate. The corresponding zero-point energies are listed in the last column (eV).

	$\omega_x(cm^{-1})$	$\omega_y(cm^{-1})$	$\omega_z(cm^{-1})$	$\frac{1}{2}\Sigma_i\ \omega_i$(eV)
IS_0'(hcp)	766	756	641	0.134
TS_1'	1112	815	**Im**	0.119
IS′(fcc)	745	752	706	0.137
TS_2'	745	733	**Im**	0.092
FS_0'	471	435	404	0.081
TS_3'	1085	1050	**Im**	0.132
FS′	417	344	328	0.068
Bulk	299	323	329	0.059

"A" in Fig. 1) in Mg(0001) using a static Mg-matrix, obtaining an activation energy of 0.15 eV—excluding vibrational contributions.

In order to simulate the diffusion of individual hydrogen atoms into the magnesium, only one hydrogen atom is left in the unit cell; it is initially placed in a hcp site (IS_0'). The energy difference between the fcc and hcp sites is found to be 20 meV, which compares well with the 25 meV obtained by Jacobson *et al.*[30] Following the reaction coordinate in Fig. 4, the barrier for surface diffusion from IS_0' to IS′ (on top of the fcc-channel) is found to be $E_1=0.14$eV; further diffusion into the magnesium is found to occur via this channel. Continuing along the reaction coordinate (i.e., down the fcc-channel), a second transition state (TS_2') is encountered, with a corresponding activation energy of $E_2'=0.53$ eV. Moving to FS_0', the energy is lowered by 0.17 eV, and the activation energy of TS_3' is 0.18 eV. At FS′, the energy is only 0.02 eV lower than at FS_0'; hence surface effects are minimal. From the sub-surface site to the octahedral, bulk-like fcc-site (FS′), the activation energy for diffusion yields a value of $E_3'=0.18$ eV (the corresponding vibrational frequencies are found in Table II).

A. Interstitial hydrogen in bulk Mg

For comparison, a bulk calculation using a super cell consisting of 36 Mg atoms in a $(3\times3\times4)$ configuration and one hydrogen atom—where all atoms are allowed to relax their positions—has also been performed.

The atomic relaxations of the neighboring Mg atoms to accommodate the hydrogen atom are very small (~0.02 Å), and the electronic *embedding density* at the position of the hydrogen atom (the octahedral site)—set-up by the surrounding Mg atoms—is found to be close to the optimum value for hydrogen, i.e., $0.012-e/a_0^{-3}$.[31]

The resulting vibrational frequencies are close to those found for an H atom in FS′ (see Table II), leading to the conclusion that the slab is sufficiently thick to emulate bulk conditions and the surface super cell is large enough to obtain realistic frequencies.

The bulk calculation yields a heat of solution for H-atoms in bulk hcp structured magnesium of $\Delta H°=0.22$ eV (including the difference in zero-point energy), which is in excellent agreement with experimental results; see, e.g., Zeng *et al.*[32]

B. Vibrational frequencies

The vibrational frequencies of the diffusing hydrogen atom in all the local minima and transition states are listed in Table II.

The zero-point energies are seen to vary by up to 64 meV between initial, transition, and final states. Such changes are substantial, when compared to an outward diffusion barrier $E_3''=E'_{TS_3}-E'_{FS}=0.18$ eV, causing an increase in the barrier of 35%.

The calculated frequencies are in good agreement with those obtained by Hjelmberg on Mg(0001)—who only calculated frequencies for the most symmetric position.[33]

The large zero-point contributions at the bulk-like transition state TS_3' is a consequence of the motion of the atom being restricted by the saddle point in configuration space.

VI. SUMMARY

The potential energy surface for the interaction of hydrogen with Mg(0001) is found to display large activation energies for the dissociation of H_2 and the first layer diffusion of atomic hydrogen into the Mg-matrix. An analysis of the relevant rates involved in the ab- and desorption is presented in the following using classical and quasi-classical harmonic transition state theory.

TABLE III. The calculated classical prefactors, classical/quasi-classical activation energies, and corresponding rates at ambient conditions (RT=20°C and 1 bar) and high temperature HT=300°C, for the hydrogen absorption processes.

	$\frac{1}{2\pi}\frac{\Pi_i\ \omega_i^{IS}}{\Pi_i'\ \omega_i^{TS}}$ (s^{-1})	E_a (eV)	E^* (eV)	$r_{cl.}$(RT) (s^{-1})	r_q(RT) (s^{-1})	r_q(HT) (s^{-1})
H_2 diss.	(2.6×10^6)	1.15	1.07	4.4×10^{-14}	1.6×10^{-11}	6.5×10^{-3}
$D_1(TS_1')$	2.0×10^{12}	0.14	0.12	7.7×10^{9}	4.9×10^{10}	7.5×10^{11}
$D_2(TS_2')$	3.5×10^{12}	0.53	0.49	2.7×10^{3}	2.2×10^{4}	4.9×10^{8}
$D_3(TS_3')$	3.5×10^{11}	0.18	0.23	2.8×10^{8}	4.7×10^{8}	3.8×10^{10}

TABLE IV. The calculated classical prefactors, classical/quasi-classical activation energies, and corresponding rates at ambient conditions (RT=20°C and 1 bar) and high temperature HT=300°C, for the hydrogen desorption processes.

	$\frac{1}{2\pi}\frac{\Pi_i \omega_i^{IS}}{\Pi_i' \omega_i^{TS}}$ (s^{-1})	E_a (eV)	E^* (eV)	$r_{cl.}$(RT) (s^{-1})	r_q(RT) (s^{-1})	r_q(HT) (s^{-1})
H_2 des.	6.0×10^{12}	1.11	1.05	4.9×10^{-7}	5.4×10^{-6}	6.1×10^{3}
$D_1'(TS_1')$	2.1×10^{12}	0.16	0.14	3.7×10^{9}	2.3×10^{10}	5.1×10^{11}
$D_2'(TS_2'')$	7.2×10^{11}	0.17	0.18	8.6×10^{8}	3.6×10^{9}	1.3×10^{11}
$D_3'(TS_3'')$	2.0×10^{11}	0.19	0.26	1.1×10^{8}	1.2×10^{8}	1.5×10^{10}
Bulk D.	1.3×10^{11}	0.19	0.27	7.2×10^{7}	6.9×10^{7}	9.6×10^{9}

A. Rates of activated processes

The flux of H_2 molecules hitting the surface per bridge site under ambient conditions ($P=1$ bar and $T=293.15$ K) is $F=3.3\times10^{8}$ site^{-1} s^{-1}. Under these conditions, given the dissociative sticking coefficient determined by Eq. (9), a quasi-classical activation energy $E_1^*=1.07$ eV (the NEB barrier including corrections for the zero-point energy), and a quantum TS_1 partition function (calculated using the frequencies from Table I), only 1.6×10^{-11} molecules site^{-1} s^{-1} will dissociate (see Table III).

From Eqs. (4) and (9) the harmonic transition state reaction rates of the diffusion processes are obtained using classical and quantum partition functions, respectively. The calculated rates of the activated hydrogen ab- and desorption processes are presented in the following.

B. Hydrogen absorption rates

The rates for the adsorption and atomic diffusion processes are calculated at ambient and high temperature conditions.

From Table III, it is clear that even if E_1^* (H_2 diss.) and $E_2^{*\prime}$ (D_2) had been comparable, the vast difference in entropic prefactors would still make the H_2 dissociation process rate-limiting. This is a natural consequence of the initial configuration being in the gas phase, and results in a rate of H_2 dissociation which is several orders of magnitude lower than for the diffusion processes. Neither the higher order temperature dependence in the dissociative prefactor, nor a geometric factor of four (two H atoms are created per dissociation and there are twice as many bridge- as fcc sites) can change that dissociation of H_2 is the rate-limiting step.

C. Hydrogen desorption rates

For the desorption processes, the hydrogen recombination is found to be rate-limiting; no other process is comparable, since the last barrier for out-wards diffusion to the surface is low (see Table IV). The meta stable state ("Meta": in Fig. 3) will not affect the barrier hydrogen recombination. In the calculation of the bulk diffusion rate ("Bulk D." in Table IV), the vibrational frequencies of the transition state TS_3' have been applied. This results in a constant for bulk self diffusion in the fcc-channel of $D_{300\ K}=(\ell^2/2)\cdot r_q=2.2\times10^{-12}$ m^2/s, which is in good agreement with the experiments by Renner and Grabke.[8]

In summary, the classical rates for ab- and desorption are found to be within an order of magnitude of the quasi-classical rates, at temperatures $\geqslant$RT, and the kinetics are found not to be diffusion limited—in agreement with, e.g., Töpler *et al.* who showed the increased kinetics in Mg_2Ni compared to Mg is a consequence of surface effects, not improved hydrogen diffusion.[9]

VII. CONCLUSION

The calculations have shown that the dissociation and recombination of H_2 are the rate-limiting processes in ab- and desorption of hydrogen at the magnesium(0001) surface. The determined dissociation and recombination barriers are significantly higher than predicted in previous LDA calculations, but in light of the excellent agreement with experiments obtained here for the desorption barrier, vibrational frequencies, heat of solution, and diffusion constants, this is seen as a consequence of the LDA overbinding.

It is found to be highly unlikely that, e.g., surface corrugation or steps will make either sorption process diffusion limited; for this to happen a catalyst must be added.

Contributions from the zero-point energy are found to be substantial for the atomic diffusion processes, where barriers are otherwise underestimated by up to 1/3. However, simply adding the zero-point energy to the classical barrier results in an overcompensation.

The agreement with experimental values for bulk diffusion and hydrogen surface frequencies is an indication that the harmonic approximation can be applied outside the low temperature regime.

ACKNOWLEDGMENTS

The author wishes to thank Professor Jens K. Nørskov and Professor Karsten W. Jacobsen for helpful discussions. The present work is financed by the Danish Research Agency and Danfoss Corporate Ventures A/S through Grant No. 2013-01-0043. The Center for Atomic-scale Materials Physics (CAMP) is sponsored by the Danish National Research Foundation.

[1] L. Schlapbach and A. Züttel, Nature (London) **414**, 353 (2001).
[2] R. B. Schwarz, MRS Bull. **24**, 40 (1999).
[3] N. Gérad and S. Ono, Chap. 4 in *Hydrogen in Intermetallic Compounds II. Topics in Applied Physics*, edited by L. Schlapbach (Springer, Berlin, 1992), Vol. 67, p. 165.
[4] J. K. Nørskov, A. Houmøller, P. K. Johansson, and B. I. Lundquist, Phys. Rev. Lett. **46**, 257 (1981).
[5] D. M. Bird, L. J. Clarcke, M. C. Payne, and I. Stich, Chem. Phys. Lett. **212**, 518 (1993).
[6] P. T. Sprunger and E. W. Plummer, Chem. Phys. Lett. **187**, 559 (1991).
[7] P. T. Sprunger and E. W. Plummer, Surf. Sci. **307**, 118 (1994).
[8] J. Renner and H. J. Grabke, Z. Metallkd. **69**, 639 (1978).
[9] J. Töpler, H. Buchner, H. Säufferer, K. Knorr, and W. Prandl, J. Less-Common Met. **88**, 397 (1982).
[10] P. Spatz, A. Aebischer, A. Krozer, and L. Sclacpbach, Z. Phys. Chem. (Munich) **181**, 955 (1993).
[11] B. Hammer and O. H. Nielsen, in *Workshop on Applied Parallel Computing in Physics, Chemistry, Engineering Science (PARA95)*, Vol. 1041 of Springer Lecture Notes in Computer Science, edited by J. Wasniewski (Springer, Berlin, 1995).
[12] DACAPO pseudopotential code. URL http://www.fysik.dtu.dk/campos
[13] D. Vanderbilt, Phys. Rev. B **41**, 7892 (1990).
[14] B. Hammer, L. B. Hansen, and J. K. Nørskov, Phys. Rev. B **59**, 7413 (1999).
[15] H. J. Monkhorst and J. D. Pack, Phys. Rev. B **13**, 5188 (1976).
[16] G. Kresse and J. Furthmuller, Comput. Mater. Sci. **6**, 15 (1996).
[17] P. Staikov and T. Rahman, Phys. Rev. B **60**, 016613 (1999).
[18] P. Hänggi, P. Talkner, and M. Borkovec, Rev. Mod. Phys. **62**, 251 (1990); A. F. Voter and J. Doll, J. Chem. Phys. **82**, 80 (1985).
[19] H. Brune, Surf. Sci. Rep. **31**, 121 (1998); T. Itoh, G. R. Bell, A. R. Avery, T. S. Jones, B. A. Joyce, and D. D. Vvedensky, Phys. Rev. Lett. **81**, 633 (1998); C. L. Liu, J. M. Cohen, J. B. Adams, and A. F. Voter, Surf. Sci. **253**, 334 (1991).
[20] G. Boisvert, N. Mousseau, and L. J. Lewis, Phys. Rev. B **58**, 12667 (1998); U. Kürpick and T. S. Rahman, Surf. Sci. **427**, 15 (1999).
[21] T. Vegge, T. Rasmussen, T. Leffers, O. B. Pedersen, and K. W. Jacobsen, Phys. Rev. Lett. **85**, 3866 (2000).
[22] J. Jørgen Mortensen, "A theoretical study of adsorption and dissociation on metal surfaces," Ph.D. thesis, Technical University of Denmark, 1998.
[23] G. Mills, H. Jónsson, and G. Schenter, Surf. Sci. **324**, 305 (1995); H. Jónsson, G. Mills, and K. W. Jacobsen, *Classical and Quantum Dynamics in Condensed Phase Simulations*, edited by B. J. Berne, G. Ciccotti, and D. F. Coker (World Scientific, Singapore, 1998).
[24] G. Henkelman and H. Jónsson, J. Chem. Phys. **113**, 9978 (2000); G. Henkelman, B. P. Uberuage, and H. Jónsson, *ibid.* **113**, 9901 (2000).
[25] T. Vegge, T. Leffers, O. B. Pedersen, and K. W. Jacobsen, Mater. Sci. Eng., A **319–321**, 119 (2001).
[26] A. Gross and M. Scheffler, J. Vac. Sci. Technol. A **15**, 1624 (1997).
[27] J. R. Kitchin, "Tuning the electronic and chemical properties of metals: Bimetallics and transition metal carbides," Ph.D thesis, University of Delaware, 2004.
[28] S. Kurth, J. P. Perdew, and P. Blaha, Int. J. Quantum Chem. **75**, 889 (1999).
[29] W. Kohn, Rev. Mod. Phys. **71**, 1253 (1999).
[30] N. Jacobson, B. Tegner, E. Schröder, P. Hyldgaard, and B. I. Lundquist, Comput. Mater. Sci. **24**, 273 (2002).
[31] J. K. Nørskov and F. Besenbacher, J. Less-Common Met. **130**, 475 (1987).
[32] K. Zeng, T. Klassen, W. Oelerich, and R. Bormann, Int. J. Hydrogen Energy **24**, 989 (1999).
[33] H. Hjelmberg, Surf. Sci. **81**, 539 (1979).